HHS Public Access

Author manuscript

Dev Neurosci. Author manuscript; available in PMC 2017 January 06.

Published in final edited form as:

Dev Neurosci. 2016 ; 38(1): 1–14. doi:10.1159/000441943.

Translating adult electrophysiology findings to younger patient populations: difficulty measuring 40 Hz auditory steady-state responses in typically developing children and children with autism spectrum disorder

J. Christopher Edgar[1], **Charles L. Fisk IV**[1], **Song Liu**[1], **Juhi Pandey**[2], **John D. Herrington**[2], **Robert T. Schultz**[2], and **Timothy P.L. Roberts**[1]

[1]Department of Radiology, Children's Hospital of Philadelphia, Philadelphia, PA, USA

[2]Center for Autism Research, Department of Pediatrics, Children's Hospital of Philadelphia, Philadelphia, PA, USA

Abstract

Background—Gamma (~30 to 80 Hz) brain rhythms are thought to be abnormal in neurodevelopmental disorders such as schizophrenia (SZ) and autism spectrum disorder (ASD). In adult populations, auditory 40 Hz click trains or 40 Hz amplitude-modulated tones are used to assess the integrity of superior temporal gyrus (STG) 40 Hz gamma-band circuits. As STG 40 Hz auditory steady-state responses (ASSRs) are not fully developed in children, tasks using these stimuli may not be optimal in younger patient populations. The present study examined this issue in typically developing (TD) children as well as in children with ASD, using source localization to directly assess activity in the principal generators of the 40 Hz ASSR - left and right primary/secondary auditory cortex.

Methods—40 Hz amplitude-modulated tones of 1sec duration were binaurally presented while magnetoencephalography (MEG) data were obtained from forty-eight TD children (45 males; 7- to 14-years-old) and forty-two children with ASD (38 males; 8- to 14-years-old). T1-weighted structural MRI was obtained. Using single dipoles anatomically constrained to each participant's left and right Heschl's Gyrus, left and right 40 Hz ASSR total power (TP) and inter-trial coherence (ITC) measures were obtained. Associations between 40 Hz ASSR TP, ITC and age as well as superior temporal gyrus (STG) gray matter cortical thickness were measured. Group STG function and structure differences were also examined.

Results—TD and ASD groups did not differ on 40 Hz ASSR TP or ITC. In TD and ASD, age was associated with left and right 40 Hz ASSR ITC ($p < 0.01$). The interaction term was not significant, indicating in both groups a ~0.01/year increase in ITC. 40 Hz ASSR TP and ITC were greater in the right than left STG. Groups did not differ in STG cortical thickness, and no associations were observed between 40 Hz ASSR activity and STG cortical thickness. Finally, right STG transient gamma (50 to 100 ms and 30 to 50 Hz) was greater in TD versus ASD (significant for TP, trend for ITC).

((Corresponding Author)), J. Christopher Edgar, PhD, Department of Radiology, Children's Hospital of Philadelphia, 34th and Civic Center Blvd, Wood Building, Suite 2115, Philadelphia, PA 19104 (USA), Tel: 215-590-3573, edgarj@email.chop.edu.

Conclusions—The 40 Hz ASSR develops, in part, via an age-related increase in neural synchrony. Greater right than left 40 Hz ASSRs (ITC and TP) suggested earlier maturation of right versus left STG neural network(s). Given a ~0.01/year increase in ITC, 40 Hz ASSRs were weak or absent in many of the younger participants, suggesting that 40 Hz driving stimuli are not optimal for examining STG 40 Hz auditory neural circuits in younger populations. Given the caveat that 40 Hz auditory steady-state neural networks are poorly assessed in children, present analyses do not point to atypical development of STG 40 Hz ASSRs in higher-functioning children with ASD. Although groups did not differ on 40 Hz auditory steady-state activity, replicating previous studies, there was evidence for greater right STG transient gamma activity in TD versus ASD.

Keywords

autism spectrum disorder; auditory steady-state response; gamma; development

Introduction

Gamma-band abnormalities (~30 to 80 Hz) are hypothesized to contribute to brain dysfunction and clinical symptoms in psychiatric disorders such as schizophrenia (SZ(1)), autism spectrum disorder (ASD(2, 3)), and attention-deficit hyperactivity disorder (ADHD(4)). In SZ, whereas increased resting-state gamma power has been reported in resting-state studies (for a review see (1)), decreased task-related gamma activity has been reported in perceptual closure tasks (5-7) and face processing tasks(8). Similar findings have been observed in ASD (for a recent review, see (2)). For example, whereas increased gamma in ASD has been reported in resting-state studies (9, 10), decreased task-related gamma activity has been reported in perceptual closure tasks (11) and face processing tasks (12). Researchers speculate that treatments normalizing gamma rhythms will lead to clinical improvement. Behavioral (13) and pharmacological studies (4, 14) have provided some support for this claim.

Across disorders, gamma abnormalities are thought to reflect synaptic and local circuit dysfunction, with gamma abnormalities due, in part, to abnormal excitatory/inhibition balance in cortical microcircuits (15). At the local circuit level, gamma activity is generated through feedback inhibition on pyramidal neurons by synaptically and electrically connected networks of fast-spiking interneurons expressing the calcium-binding protein parvalbumin (PV) (16). Recent optogenetic studies have shown that activation of PV interneurons is both necessary and sufficient to generate gamma oscillations in the mammalian cortex, which in turn regulates cortical information processing (17). These studies have demonstrated that an increase in the excitatory input to these fast-spiking interneurons via selective optogenetic stimulation leads to an increase in gamma activity. Although the precise network and synaptic mechanisms underlying these effects remain unclear (18), phasic inhibition mediated by fast-spiking interneurons appears to be to the driving force behind gamma oscillations (19), as opposed to tonic GABA(A) agonist application. Further details regarding the generation of gamma cortical rhythms are described in a recent review (20).

Brain neural activity is non-invasively assessed using electroencephalography (EEG) or magnetoencephalography (MEG). EEG and MEG activity is typically examined in frequencies ranging from delta (1 to 4 Hz) to gamma (~30 to 80 Hz). Theta and delta activity is sometimes easier to record compared to gamma activity as the strength of neural activity is inversely proportional to frequency. A strategy to increase the gamma signal has been to 'drive' gamma networks. In the auditory system, this is often accomplished using auditory 40 Hz steady-state stimuli: 40 Hz click trains or 40 Hz amplitude-modulated tones. In adults, primary/secondary auditory cortex neurons entrain best to 40 Hz stimuli versus other driving frequencies (21-25). Almost all studies examining 40 Hz auditory steady-state responses (ASSRs) in SZ have reported abnormalities (21-26), and the few studies examining 40 Hz ASSRs in ASD or ASD family members have also observed abnormalities (27, 28).

Although in adults 40 Hz click trains and 40 Hz amplitude-modulated tones produce 40 Hz ASSRs that are easily measured, there is evidence that 40 Hz auditory steady-state stimuli do not produce measurable driving responses in infants and children. For example, Maurizi et al.(29) observed poor test-retest 40 Hz ASSR reliability in 32 full-term newborns and in 10 children aged 5- to 8-years-old, and Stapellis et al.(30) saw no clear 40 Hz ASSR in infants aged 3 weeks to 28 months. Aoyagi et al.(31), examining sedated subjects, showed that in young children the 40 Hz ASSR is difficult to elicit, becoming increasingly detectable from 6 months to 15 years. Using MEG to examine 40 Hz ASSRs in sixty-nine healthy participants aged five to fifty-two years, Rojas et al.(32) concluded that full development of left and right hemisphere 40 Hz ASSR neural generators are not complete until early adulthood. Examining 188 individuals aged 8 to 22, Cho et al.(33) observed 40 Hz ASSRs evoked power and phase-locking increasing from 8 to 16 years, and then decreasing towards ages twenty-two. Increases in the strength of the 40 Hz ASSR were especially marked between the late childhood group (8-10 years) and the early-adolescence group (11-13 years). The decrease in 40 Hz ASSR in the early adulthood group (20-22 years) versus the younger groups is consistent with Edgar et al.(26), who observed a linear decreases in the strength of 40 Hz ASSRs from 21 to 58 years, with approximately 15% of the decrease in 40 Hz ASSRs associated with normal age-related decreases in gray matter cortical thickness. Finally, in the only longitudinal study, Poulsen et al.(34) examined changes in 40 Hz ASSRs in adolescence at two time points – ages 10 and 11.5 years. Poulsen et al. observed larger left and right 40 Hz ASSRs at 11.5 versus 10 years of age. Comparing the 11.5 year olds to adults, no differences in STG 40 Hz ASSR source strength were observed. Although the Poulsen et al. findings differ somewhat from Rojas et al.(32) and Cho et al.(33) as they suggest that full development of the 40 Hz ASSR may be observed during early adolescence rather than early adulthood, research in this area generally indicates that 40 Hz ASSRs are not easily recorded in younger populations. Thus, although there is a move in the field to conduct imaging studies in young populations in order to understand brain abnormalities prior to and at the onset of disease, the use of 40 Hz auditory steady-state tasks to examine auditory gamma activity may not be as useful in these populations.

The present study further explored this issue, examining a large number of typically developing (TD) participants 7- to 14-years-old to estimate changes from childhood to early adolescence. Given that Heschl's Gyrus is the primary generator of the magnetic 40 Hz

ASSR (e.g., (35-37)), 40 Hz ASSR activity was estimated from sources anatomically constrained to each participant's Heschl's Gyrus to obtain an optimal estimate of gamma activity even in the presence of low signal. Furthermore, given that a previous study showed associations between 40 Hz auditory steady-state activity and STG gray-matter in adults (26), STG gray-matter cortical thickness measures were obtained and function-structure associations examined. Finally, given putative 40 Hz abnormalities in adults with ASD, we hypothesized that a sample of ASD youth would show decreased total power and decreased intertrial coherence (ITC) in the 40 Hz ASSR relative to the TD group.

Methods and materials

2.1 Participants

MEG data were obtained from fifty-six TD children (53 males; 7- to 14-years-old) and fifty-five children with ASD (51 males; 8- to 14-years-old). Of these 111 participants, MEG data were lost due to insufficient trials (fewer than 50 trials (N = 6)), noisy MEG data due to metal artifacts (N = 2), MEG technical problems (N = 6), or no M50 response in the left and right hemisphere, perhaps suggesting auditory stimuli were not adequately heard (N = 7). The demographics and results reported below are for the evaluable sample of 48 TD and 42 ASD participants.

All participants were selected according to the following criteria: 1) no history of traumatic brain injury or other significant medical or neurological abnormality, 2) no active psychosis, 3) no MRI contraindications, and 4) no known drug or alcohol use within 24 hours of any of study procedures. Members of the TD group were evaluated by licensed clinical psychologists who ruled out the presence of DSM-IV-TR Axis I disorders based on clinical judgment, review of the child's medical history form and parent interview. Current diagnosis of ASD was confirmed by expert clinical judgment based on NIH CPEA guidelines, including the Autism Diagnostic Observation Schedule - Generic (38) and Autism Diagnostic Interview - Revised (39) and with consensus diagnostic agreement between at least two experienced clinicians. Additional details on participant recruitment procedures are provided in Edgar et al. (31).

In the ASD group, 15 participants were being treated with ADHD medications (e.g., Concerta, Strattera), 3 participants treated with 2nd generation antipsychotics (e.g., Risperidone), 10 participants with antidepressants (e.g., Prozac, Sertaline), and 1 participant with anxiolytics (Buspirone). No participants in the TD group were taking psychotropic medications.

2.2 MEG and MRI data acquisition

MEG data were recorded continuously using a 306-channel Vector-View system (Elekta-Neuromag, Helsinki, Finland) with a sampling rate of 1000 Hz and a bandpass of 0.1 to 330 Hz. Electro-oculogram (EOG) (vertical EOG on the upper and lower left sides) and electrocardiogram (ECG) were also obtained. The participants' head position was monitored using four head position indicator (HPI) coils attached to the scalp.

The amplitude of a 500 Hz tone of 1 second duration was modulated at 40Hz (modulation depth 100%), binaurally presented with a 4 second ISI (±2 seconds), and delivered using a sound pressure transducer through conduction tubing to the ear canal via ear-tip inserts (ER3A, Etymotic Research, IL, USA). Prior to data acquisition, 500 Hz tones of 300 ms duration and 10 ms rise time were used to obtain auditory thresholds for each ear. Auditory thresholds were initially estimated via stepwise amplitude reduction until participants stopped verbally identifying the presence of the tone. For fine tuning, tone loudness was then adjusted within +/− 10 dB of the preliminary threshold until a final threshold was confirmed (approximately 50% accuracy). For the 40 Hz steady-state task, for each ear, the peak intensity of the steady-state stimuli was presented 45 dB above each participant's hearing threshold. TD and ASD did not differ in left or right auditory threshold values (*p*s > 0.05). To minimize fatigue, during the task participants viewed (but did not listen to) a movie projected onto a screen positioned at a comfortable viewing distance.

Following the MEG task, MEG data were corrected for head motion using MaxMove™, and Maxfilter™ was used for noise reduction using a signal space separation method with a temporal extension (tSSS; (40)). After motion correction and tSSS, artifact correction was applied to remove eye-blink activity as outlined by Roberts et al.(41) using BESA. Non eye-blink artifacts were rejected by amplitude and gradient criteria (amplitude > 1200 fT/ cm, gradients > 800 fT/cm/sample). Artifact free epochs were then averaged, with MEG data analyzed only from participants with 50+ trials. The number of artifact-free trials did not differ between TD (mean = 122; SD=22) and ASD (mean =118; SD=21), t(88) = 1.04, $p > .05$.

After the MEG session, structural magnetic resonance imaging (sMRI) provided T1-weighted, 3-D anatomical images using a 3T Siemens Verio scanner (voxel size 0.8 × 0.8 × 0.9 mm).

2.3 Source Localization

To coregister MEG and sMRI data, three anatomical landmarks (nasion and right and left preauriculars) as well as an additional 200+ points on the scalp and face were digitized for each participant using the Probe Position Identification (PPI) System (Polhemus, Colchester, VT), and an affine transformation matrix that involved rotation and translation between the MEG and sMRI coordinate systems was obtained via a least-squares match of the PPI points to the surface of the scalp and face.

For all participants, measures were obtained for the left and right 40 Hz ASSR. Given weak 40 Hz ASSRs in many participants (see below), to confirm that the auditory stimuli were heard, measures for the left and right 50 ms (M50) response were also obtained. Specifically, using the 40 Hz steady-state stimuli (i.e., same task), in addition to the 40 Hz ASSR, the M50 response was examined(42, 43). As the primary generator of both the M50 response and the ASSR is well modeled by single dipoles in left and right Heschl's Gyrus and surrounding regions (e.g., (35-37, 44, 45)), source localization was performed using an anatomical constraint. Thus, after co-registering the MEG and sMRI data, each participant's left and right Heschl's Gyrus was visually identified and a dipole source placed at the ‘center’ of each Heschl's Gyrus (at an anterior to posterior midpoint, and approximately two-

thirds from the medial termination of Heschl's Gyrus; if two Heschl's Gyri were present, the dipole was placed in-between the two Heschl's Gyri). Figure 1a shows an example of left and right dipole source placement. After placing the left and right dipoles, for each participant, left- and right-STG dipoles were oriented at (1) the maximum of the M50 response, and (2) the maximum of the ASSR. Thus, estimates of left and right STG activity were obtained using an individualized anatomical constraint, with orientation of the M50 and ASSR dipoles optimized for each participant and evoked component. In particular, M50 dipole orientations were obtained after applying a 2 Hz (24B/octave, zero-phase) to 55 Hz (48dB/octave, zero-phase) band-pass filter, and 40 Hz steady-state dipole orientations (300 to 900 ms) were obtained after applying a 40Hz bandpass filter with 50% amplitude cutoff frequencies of 30 and 50 Hz (and with almost complete attenuation at 20 and 60 Hz). All source analyses were performed blind to participant group.

2.4 Source time-frequency analysis

The calculation of single-trial phase and magnitude for the left and right sources used procedures outlined in Hoechstetter et al. (46) where in each participant the derived source model was applied to the raw unfiltered data. Each source model was constructed by including left and right Heschl's Gyrus oriented sources and the eye-blink source vector derived for each participant to remove eye-blink activity (47, 48). This final source model served as a source montage for the raw MEG (49, 50). Examining the source waveforms, transformation from the time domain to the time-frequency domain used complex demodulation procedures (51) implemented in BESA, using frequencies between 4 and 56 Hz, in steps of 2 Hz. Continuous data were analyzed relative to tone onset every 25 ms (i.e., each 40 Hz cycle), utilizing +/− 39.4 ms and +/− 2.83 Hz (full width at half maximum parameters) of contiguous data at each 25 ms step.

Total power and phase-locking measures were extracted from the single-trial complex time-frequency matrix. Total power was calculated by averaging the time-frequency spectra of each MEG epoch. When pre-stimulus power is subtracted, post-stimulus total power (TP) assesses the post-stimulus increase in the magnitude/power of oscillatory activity (temporal spectral evolution, TSE). A measure of phase-locking referred to as inter-trial coherence (ITC) was also computed. Inter-trial coherence (ITC) is a normalized measure assessing the trial-to-trial similarity of oscillatory activity, with ITC=1 reflecting no phase variability and ITC=0 reflecting maximal phase variability across trials.

For the TP and ITC time–frequency t-test group comparisons, family-wise error was controlled using cluster size thresholds derived from Monte Carlo simulations (e.g., see (52, 53)). The method computes the probability of a random field of noise producing a cluster of adjacent time–frequency cells of a given size after the noise is thresholded at a given probability level and provides a corrected p-value. The cluster size needed to obtain the desired family-wise correction was determined using a standard fMRI package (AFNI AlphaSim) and clustering performed with custom MatLab software.

2.5 Cortical Thickness Measures

FreeSurfer (http://sufer.nmr.mgh.harvard.edu) uses intensity and continuity sMRI information in segmentation and deformation procedures to obtain cortical thickness (CT) measures, calculated as the closest distance from the gray/white to gray/cerebral-spinal-fluid boundary at each vertex on the tessellated surface (54). Using Freesurfer, sMRI from each participant were processed to obtain STG cortical-thickness (CT) measures using the procedures outlined in Edgar et al. (55). CT measures for Heschl's gyrus (HG), planum temporale (PT), and the lateral aspect (LA) of the STG were obtained. STG gray-matter CT data from twelve participants were excluded due to excessive motion. To reduce the chance of type I error, in each hemisphere an average left and right STG CT score was calculated (i.e., for each hemisphere: (HG + PT + LA)/3).

For all analyses, participants more than 2.5 standard deviations from the mean were excluded (typically 1 to 2 participants per analysis).

Results

3.1 Demographics

As shown in Table 1, groups did not differ in age or IQ. As expected, ASD participants had higher Social Responsiveness Scale scores (SRS (56)) than the TD participants.

3.2 Source Localization (M50 and ASSR)

Goodness-of-fit (GOF), computed using all MEG sensors, did not differ between TD and ASD for M50 (peak of response; TD mean = 70% (SD =13.5); ASD mean = 70% (SD = 14.6); $p > 0.05$) or the 40 Hz ASSR (peak from 300 to 900 ms; TD mean = 51%, SD=12.4; ASD mean = 50%, SD = 9.8, $p > 0.05$). The above M50 GOF values are similar to those observed in auditory studies using a two dipole source model and modeling activity at all MEG sensors (26, 53, 57). Exploratory hierarchical regression analyses examined associations between GOF and age (regression model with age entered 1st, group 2nd, and interaction term last). For M50, no main effects or interactions were observed (*ps* > 0.05). For 40 Hz ASSR, a main effect of age, $F(1,88) = 5.78$, $p < 0.05$, indicated larger GOF values in older than younger participants, and with a trend interaction term, $F(1,86) = 2.34$, $p = 0.13$, suggesting a stronger age-related association in TD (r= 0.37) versus ASD (0.12).

ANOVAs examined group and hemisphere differences in dipole location. No main effects or interactions were observed in the 'x' direction. In the 'y' direction, a main effect of Hemisphere, $F(1,88) = 67.75$, $p < 0.001$, indicated more posterior dipole locations in the left than right (4.09 mm difference). In the 'z' direction, simple effect analyses of a Group X Hemisphere interaction, $F(1,88) = 3.88$, $p < 0.05$, showed similarly located left and right 'z' position dipoles in TD versus more inferior left than right dipoles in ASD (2.94 mm).

In a majority of participants, 40 Hz ASSR dipole orientations were 'random' given a weak or no observable 40 Hz ASSR. As a demonstration, although the M50 and ASSR generators are thought to be similarly located and thus similarly oriented, as shown in Figure 1b, variability across participants in azimuthal dipole angle $\left(\theta = tan^{-1}\left(\frac{z\ \ component}{y\ \ component}\right)\right)$ was

much less for M50 (upper plots) than the 40 Hz ASSR (lower plots), with the more distributed 40 Hz ASSR dipole orientation pattern likely due to a weak or absent 40 Hz ASSR.

Figure 1c histograms show the difference in M50 and 40 Hz ASSR dipole orientations, in each hemisphere comparing each participant's M50 and 40 Hz ASSR orientations, comparing participants with 40 Hz ASSR GOF values ≥ 50% (N = 38; black bars) versus participants with GOF values < 50% (N = 52; gray bars). Greater similarity in dipole orientation was observed for participants with a higher versus lower ASSR GOF, indicated by the high GOF participants showing smaller differences between M50 and 40 Hz ASSR orientations.

Given that in many participants 40 Hz ASSR were weak or not present, and given anatomic similarity in M50 and ASSR generators (35-37, 58-60), 40 Hz ASSR TP and ITC estimates were obtained using the more reliable M50 source model.

3.3 Source Time-frequency Analyses

Figure 2 shows grand average TP maps for the TD (top row) and ASD groups (middle row), with uncorrected statistical maps shown in the bottom row. The region surviving familywise correction is highlighted in gray and with an '*'. No 40 Hz ASSR group differences were observed. In the left STG, from 100 to 200 ms, significantly increased 8 to 20 Hz activity was observed in ASD versus TD. Figure 3 shows grand average ITC maps for the TD (top row) and ASD groups (middle row), with uncorrected statistical maps shown in the bottom row. No pre- or post-stimulus ITC group differences survived familywise correction.

To more directly focus on the 40 Hz ASSR, repeated measures ANOVAs examined Hemisphere and Group differences for the 40 Hz ASSR, using a single 40 Hz ASSR TP and ITC measure per hemisphere and per participant, computed as the average TP or ITC in a 300 to 900 ms and 38 to 42 Hz region-of-interest. For TP, a significant main effect of Hemisphere, $F(1,88) = 3.91$, $p < 0.05$, indicated greater right than left TP. For ITC, a main effect of Hemisphere, $F(1,87) = 11.60$, $p < 0.01$, indicated greater right than left ITC. Figure 4 bar graphs show TP and ITC mean and standard error values for each group and each hemisphere. For TP and ITC, the main effect of Group and the Group X Hemisphere interaction term were not significant. Left and right TP and ITC 40 Hz ASSR effect sizes were computed. For TP, Cohen's D was 0.18 for the left and 0.24 for the right. For ITC, Cohen's D was 0.12 for the left and 0.01for the right. Effect size values indicate that the present study was not underpowered to detect 40 Hz ASSR group differences.

Finally, given previous findings of early transient gamma group differences to auditory stimuli in children and adolescents with ASD(52), and given that the uncorrected TP and ITC statistics maps suggested transient gamma group differences (i.e., right-hemisphere blue voxels between 50 and 100 ms and 30 to 50 Hz), exploratory analyses examined group differences using a single TP and ITC measure per hemisphere and per participant, computed as the average TP or ITC in a 50 to 100 ms and 30 to 50 Hz region-of-interest. Whereas left transient gamma TP in TD (mean = 0.81, SD = 5.80) did not differ from ASD (mean = 1.38, SD = 6.06; $p = 0.64$), right transient gamma TP was greater in TD (mean =

2.70, SD = 5.85) versus ASD (mean = 0.59, SD = 3.93; $p = 0.05$). For ITC, whereas left transient gamma ITC in TD (mean = 0.123, SD = 0.026) did not differ from ASD (mean = 0.124, SD = 0.028; $p = 0.80$), there was a trend for greater right transient gamma ITC in TD (mean = 0.126, SD = 0.022) versus ASD (mean = 0.119, SD = 0.02; $p = 0.11$).

3.4 Total Power and inter-trial coherence associations with age

For each hemisphere, hierarchical regressions were performed with Age entered first, Group second, the Age X Group interaction term last, and with 40 Hz TP or ITC as the dependent measure. For left TP, none of the main effects or the interaction term were significant (*p's* > 0.26). For right TP, a significant main effect of Age, $F(1,88) = 4.19$, $p < 0.05$, indicated increased right TP in older participants, with a 1.02%/year increase in TP (i.e., ~ 1% increase in baseline-corrected 40 Hz TP normalized to pre-stimulus power).

For ITC, a main effect of Age in left STG, $F(1,87) = 6.25$, $p < 0.05$, and right STG, $F(1,87) = 6.84$, $p < 0.05$, indicated greater similarity in the trial-to-trial phase of 40 Hz steady-state responses in older children, with an ~0.01/year change in ITC. The Group and Age X Group terms were not significant in either hemisphere.

Given age associations with TP and ITC in the right STG, hierarchical regression analyses, with age as the dependent variable and right TP entered first and right ITC entered second (and vice versa), examined the relative contributions of age to TP and ITC. Analyses indicated that only ITC predicted unique variance in age. Figure 5 scatterplots show associations between age and ITC for each group and each hemisphere. Figure 6 shows left and right 40 Hz ASSR evoked timecourses for a representative child from ages 7 to 13 years, demonstrating left and right STG 40 Hz ASSRs in older children versus the less evident 40 Hz ASSRs in younger children.

3.5 Associations between STG Gray-Matter Cortical Thickness and 40 Hz Total Power and ITC

A Group by Hemisphere ANOVA on STG gray-matter CT showed no main effects or interactions (*p*'s > 0.40). For gray-matter CT, a significant main effect of Age in left STG, $F(1,76) = 7.93$, $p < 0.01$, indicated decreased left STG gray-matter CT in older than younger participants ($r = -0.31$; interaction term not significant). Although the association was in the expected direction, right STG gray-matter CT was not associated with age ($r = -0.14$, $p = 0.23$). Left and right CT was not associated with left or right 40 Hz TP or ITC.

DISCUSSION

40 Hz ASSRs were not observed in the majority of participants. Analyses indicated that the development of adult-like 40 Hz ASSRs is due, in part, to increasing similarity in trial-to-trial 40 Hz responses as a function of age, with the increase in ITC estimated at ~0.01 ITC units per year. Present findings are thus consistent with Poulsen et al. (34) who, comparing 40 Hz ASSRs in same children at 10 and 11.5 years of age, observed stronger 40 Hz responses in older than younger children. Present findings, however, also support the Rojas et al.(32) observation that adult-like 40 Hz ASSRs are not reliably obtained until late adolescence or early adulthood. Given the present finding as well as other studies showing

very weak or no 40 Hz ASSRs in very young children as well as infants (29, 30), 40 Hz auditory driving tasks are not optimal for assessing the integrity of 40 HZ auditory networks non-adult populations.

It is unclear why the 40 Hz ASSR does not fully develop until early adulthood. In the present study, the observation of M50 and M100 auditory responses in almost all participants demonstrated that participants heard (and had cortical responses to) the 40 Hz auditory steady-state tones. The development of deep layers (lower layer III to layer VI) in auditory cortex occurs between 6 months and 5 years of age(61), whereas the superficial layers (upper layer III and layer II) continue to mature until about age 12 (62, 63). Based on this, researchers have hypothesized that the 50 ms auditory response reflects recurrent activation in layers III and IV, the termination zone of thalamocortical pathways that are almost fully developed by age 6. There is disagreement whether the 40 Hz ASSR is due to the superposition of transient responses (i.e., successive M50 responses or successive transient gamma responses) or is instead a true resonance phenomenon. Present findings support the latter; in particular, whereas in the this study M50 responses were observed in almost all participants, ASSRs were generally absent, lending support to the claim that the transient gamma-response (part of M50) and the ASSR are distinct. Other evidence in support of this distinction is the different behavior of the transient gamma responses and ASSR in relation to ISI(37).

Poulsen et al. (34) speculate that the late development of the ASSR indicates continued refinement in the ability of the auditory cortex to respond to rapid temporal information carried by auditory stimuli. Poulsen et al. interpreted their finding of weaker 40 Hz ASSR responses in 10-year-olds versus adults in the left but not right STG as support for this hypothesis, with these findings suggesting a more slowly (i.e., more plastic) developing language-dominant left hemisphere. In the present study, the observation of stronger 40 Hz ASSRs in the right than left STG also suggests earlier development of right than left auditory areas. Of note, however, maturation of gamma rhythms during adolescence does not appear to be specific to the auditory cortex. For example, Gaetz et al.(64) observed greater movement-related motor cortex gamma synchrony in adolescent (11- to 13-years-old) versus younger children (4- to 6-years-old), suggesting a more general phenomena. Maturation of neural oscillatory activity is, of course, observed in frequencies below gamma (e.g., (65-67)), with a recent translational study (human and rat) suggesting that increased neural synchrony may be a general feature of neural network maturation(68).

Late development of 40 Hz ASSRs could reflect incomplete development of auditory cortex areas due to continued neural pruning through late adolescents (e.g., (69)). There is also evidence that GABAergic inhibitory interneurons mature relatively late in development (70), and thus with the neural networks needed to support 40 Hz activity developing only at later stages of brain development. Whereas in the present study no associations were observed between gray-matter CT and 40 Hz ASSR total power or ITC, Edgar et al.(26) found that in healthy adult controls STG gray-matter CT accounted for ~13% of the variance in STG 40Hz ASSR total power and ~16% of the variance in 40Hz ASSR ITC. The lack of a function-structure relationship in the present study may be due to the fact that the relationships observed in Edgar et al.(26) are not observed in younger populations, perhaps

due to the fact that the gray matter changes associated with 40 Hz ASSR activity in children and adolescents, such as neural pruning and maturation of inhibitory interneurons, are largely 'invisible' to structural MRI. A lack of function-structure associations may also be due to the fact that in many participants the ASSR was weak and thus difficult to accurately measure, with 'inaccurate' ASSR TP and ITC measures precluding the ability to observe associations with gray matter. Of note, however, similar to the age and STG gray-matter correlations reported in the Edgar et al. adult group, in the present study, an association between age and left STG gray-matter cortical thickness was observed, with present findings thus consistent with Gogtay et al. (71) who showed gray-matter cortical thickness decreases in children and adolescents.

In the present study, given that 40 Hz ASSRs were weak and thus in a majority of participants it was not possible to obtain optimal orientation for the 40Hz ASSR, 40 Hz ASSR TP and ITC measures were obtained using the M50 oriented dipoles. As previously noted, given that the STG areas generating the M50 and 40 Hz ASSR are spatially close (37), M50 sources provided a reasonable estimate of 40 Hz ASSR activity. In addition, comparison of M50 and ASSR dipole orientations in the participants showing a stronger 40 Hz ASSR (as estimated by higher GOF), showed M50 and 40 Hz ASSR dipole orientations were similar, providing additional support for using the M50 sources to model 40 Hz steady-state activity. In fact, present findings indicate that the use of anatomical constraints with M50 oriented sources may be an optimal approach, as the use of single dipole or distributed source localization routines to localize 40 Hz ASSRs in children and adolescents are not likely to succeed in a majority of younger participants given weak ASSRs. A similar observation was made by Rojas et al. (32) - in a large number of the typically developing participants (~30%) ASSR signal-to-noise ratios were deemed insufficient for source localization, with most of the participants excluded from source localization being the youngest participants (personal communication).

In contrast to study hypotheses and prior findings, and given the strong caveat that 40 Hz auditory steady-state neural networks are not fully developed and are thus are poorly assessed in children and adolescents, present findings did not indicate 40 Hz ASSR abnormalities in this group of children with ASD. Indeed, children with ASD showed the same rate of development of the ASSR as controls, with regressions showing in TD and ASD a ~0.01/year increase in ITC. Present findings thus differ from Wilson et al. (27) who observed decreased left 40 Hz ASSRs in children with ASD than TD. Differences between the present study and Wilson et al. are perhaps due to the fact that Wilson et al. examined a group of children with ASD (mean age = 12.35 years; SD = 3.02) slightly older than the children with ASD in the present study (mean age = 10.6 years, SD 1.5) and thus a population with slightly stronger ASSRs. Study differences may also be due to the fact that Wilson et al. examined a more impaired group of children with ASD (mean IQ = 92; SD = 25) than the children with ASD in the present study (mean IQ = 107 years, SD = 23). Although differences may also be due to the fact that the present study used 40 Hz amplitude-modulated tones and Wilson et al. used 40 Hz click trains, the weak click train 40 Hz ASSRs in children and adolescents reported in Rojas et al. (32) suggests that study differences are not due to stimuli differences.

Although groups did not differ on 40 Hz auditory steady-state activity, there was evidence for group differences in transient gamma activity (50 to 100 ms, 30 to 50 Hz), with transient gamma TP and ITC (trend) group differences observed in the right STG. Present findings thus generally replicate Edgar et al.(52), with less prominent findings in the present study perhaps due to examining a slightly younger population in the present study than in Edgar et al. (participants examined in Edgar et al.(52) and in the present study were completely distinct populations). Indeed, a recent longitudinal study showed TD and ASD gamma group differences were more prominent in older than younger populations(72).

Finally, although not a focus of the study, time-frequency analyses showed increased left STG 100 to 200 ms post-stimulus 8 to 12 Hz TP in ASD versus TD. This finding likely reflects a delay in ASD in the typical maturational decrease in the strength of later auditory responses such as the M200.

Limitations

Although the MEG data were eye-blink corrected and trials with large amplitude and gradient artifacts removed, it is possible that low-amplitude muscle artifact contaminated auditory cortex gamma measures. This, however, is considered unlikely, given that this was a passive task and thus no task-related muscle artifact (as such, there was no need to collect neck or jaw activity using electrodes(73)), and the examination of gamma activity in source space helped to improve signal as well as reduce muscle-related artifact (74, 75). Two additional points are of note: (1) contamination of gamma activity by muscle is primarily a problem when examining non-phase-locked or induced activity (e.g., visual gamma-band studies) versus the highly phase-locked 40 Hz steady-state gamma response, and (2) contamination of gamma from microsaccades is more a problem in visual versus auditory studies. Finally, it is of note that although studies show significantly larger 40 Hz ASSRs to attended than unattended sounds (76-78), Herdman (79) found that attention to 40 Hz auditory steady-state stimuli modulated the 40 Hz ASSR in adults but not children (~12-years-old).

Conclusions

The 40 Hz ASSR develops, in part, via an age-related increase in neural synchrony. Given a ~0.01/year increase in ITC, 40 Hz ASSRs were weak or absent in many of the younger participants, suggesting that 40 Hz driving stimuli are not optimal for examining STG 40 Hz auditory neural circuits in younger populations. Given the caveat that 40 Hz auditory steady-state neural networks are poorly assessed in children, present analyses do not point to atypical development of STG 40 Hz ASSRs in higher-functioning children with ASD. Although groups did not differ on 40 Hz auditory steady-state activity, replicating previous studies, there was evidence for greater right STG transient gamma activity in TD versus ASD (50 to 100 ms, 30 to 50 Hz).

Acknowledgements

This study was supported in part by NIH Grant R01DC008871 (TR), RC1MH08879 (RTS), a NIH Grant R21NS090192 (JCE), a Grant from the Pennsylvania Department of Health (SAP # 4100042728 to RTS), and a IDDRC grant to CHOP (U54 HD08694). Dr. Roberts gratefully acknowledges the Oberkircher Family for the Oberkircher Family Chair in Pediatric Radiology at CHOP.

References

1. Gandal MJ, Edgar JC, Klook K, Siegel SJ. Gamma synchrony: towards a translational biomarker for the treatment-resistant symptoms of schizophrenia. Neuropharmacology. 2012; 62(3):1504–1518. [PubMed: 21349276]
2. Rojas DC, Wilson LB. gamma-band abnormalities as markers of autism spectrum disorders. Biomarkers in medicine. 2014; 8(3):353–368. [PubMed: 24712425]
3. Gandal MJ, et al. Validating gamma oscillations and delayed auditory responses as translational biomarkers of autism. Biological psychiatry. 2010; 68(12):1100–1106. [PubMed: 21130222]
4. Wilson TW, Wetzel MW, White ML, Knott NL. Gamma-frequency neuronal activity is diminished in adults with attention-deficit/hyperactivity disorder: a pharmaco-MEG study. Journal of psychopharmacology. 2012; 26(6):771–777. [PubMed: 22219219]
5. Spencer KM, et al. Neural synchrony indexes disordered perception and cognition in schizophrenia. Proceedings of the National Academy of Sciences of the United States of America. 2004; 101(49): 17288–17293. [PubMed: 15546988]
6. Spencer KM, et al. Abnormal neural synchrony in schizophrenia. The Journal of neuroscience : the official journal of the Society for Neuroscience. 2003; 23(19):7407–7411. [PubMed: 12917376]
7. Uhlhaas PJ, Phillips WA, Mitchell G, Silverstein SM. Perceptual grouping in disorganized schizophrenia. Psychiatry research. 2006; 145(2-3):105–117. [PubMed: 17081620]
8. Lee SH, Kim DW, Kim EY, Kim S, Im CH. Dysfunctional gamma-band activity during face structural processing in schizophrenia patients. Schizophrenia research. 2010; 119(1-3):191–197. [PubMed: 20303713]
9. Orekhova EV, et al. Excess of high frequency electroencephalogram oscillations in boys with autism. Biological psychiatry. 2007; 62(9):1022–1029. [PubMed: 17543897]
10. Cornew L, Roberts TP, Blaskey L, Edgar JC. Resting-state oscillatory activity in autism spectrum disorders. Journal of autism and developmental disorders. 2012; 42(9):1884–1894. [PubMed: 22207057]
11. Grice SJ, et al. Disordered visual processing and oscillatory brain activity in autism and Williams syndrome. Neuroreport. 2001; 12(12):2697–2700. [PubMed: 11522950]
12. Khan S, et al. Local and long-range functional connectivity is reduced in concert in autism spectrum disorders. Proceedings of the National Academy of Sciences of the United States of America. 2013; 110(8):3107–3112. [PubMed: 23319621]
13. Popov T, Rockstroh B, Weisz N, Elbert T, Miller GA. Adjusting brain dynamics in schizophrenia by means of perceptual and cognitive training. PloS one. 2012; 7(7):e39051. [PubMed: 22815697]
14. Heinrichs-Graham E, et al. Pharmaco-MEG evidence for attention related hyper-connectivity between auditory and prefrontal cortices in ADHD. Psychiatry research. 2014; 221(3):240–245. [PubMed: 24495532]
15. Rubenstein JL, Merzenich MM. Model of autism: increased ratio of excitation/inhibition in key neural systems. Genes, brain, and behavior. 2003; 2(5):255–267.
16. Tamas G, Buhl EH, Lorincz A, Somogyi P. Proximally targeted GABAergic synapses and gap junctions synchronize cortical interneurons. Nature neuroscience. 2000; 3(4):366–371. [PubMed: 10725926]
17. Cardin JA, et al. Driving fast-spiking cells induces gamma rhythm and controls sensory responses. Nature. 2009; 459(7247):663–667. [PubMed: 19396156]
18. Tiesinga P, Sejnowski TJ. Cortical enlightenment: are attentional gamma oscillations driven by ING or PING? Neuron. 2009; 63(6):727–732. [PubMed: 19778503]
19. Bartos M, Vida I, Jonas P. Synaptic mechanisms of synchronized gamma oscillations in inhibitory interneuron networks. Nature reviews. Neuroscience. 2007; 8(1):45–56. [PubMed: 17180162]
20. Wang XJ. Neurophysiological and computational principles of cortical rhythms in cognition. Physiological reviews. 2010; 90(3):1195–1268. [PubMed: 20664082]
21. Brenner CA, Sporns O, Lysaker PH, O'Donnell BF. EEG synchronization to modulated auditory tones in schizophrenia, schizoaffective disorder, and schizotypal personality disorder. The American journal of psychiatry. 2003; 160(12):2238–2240. [PubMed: 14638599]

22. Hamm JP, Gilmore CS, Picchetti NA, Sponheim SR, Clementz BA. Abnormalities of neuronal oscillations and temporal integration to low- and high-frequency auditory stimulation in schizophrenia. Biological psychiatry. 2011; 69(10):989–996. [PubMed: 21216392]
23. Hong LE, et al. Evoked gamma band synchronization and the liability for schizophrenia. Schizophrenia research. 2004; 70(2-3):293–302. [PubMed: 15329305]
24. Lenz D, Fischer S, Schadow J, Bogerts B, Herrmann CS. Altered evoked gamma-band responses as a neurophysiological marker of schizophrenia? International journal of psychophysiology : official journal of the International Organization of Psychophysiology. 2011; 79(1):25–31. [PubMed: 20705107]
25. Light GA, et al. Gamma band oscillations reveal neural network cortical coherence dysfunction in schizophrenia patients. Biological psychiatry. 2006; 60(11):1231–1240. [PubMed: 16893524]
26. Edgar JC, et al. Cortical thickness as a contributor to abnormal oscillations in schizophrenia? NeuroImage. Clinical. 2014; 4:122–129. [PubMed: 24371794]
27. Wilson TW, Rojas DC, Reite ML, Teale PD, Rogers SJ. Children and adolescents with autism exhibit reduced MEG steady-state gamma responses. Biological psychiatry. 2007; 62(3):192–197. [PubMed: 16950225]
28. Rojas DC, et al. Transient and steady-state auditory gamma-band responses in first-degree relatives of people with autism spectrum disorder. Molecular autism. 2011; 2:11. [PubMed: 21729257]
29. Maurizi M, et al. 40-Hz steady-state responses in newborns and in children. Audiology : official organ of the International Society of Audiology. 1990; 29(6):322–328. [PubMed: 2275647]
30. Stapells DR, Galambos R, Costello JA, Makeig S. Inconsistency of auditory middle latency and steady-state responses in infants. Electroencephalography and clinical neurophysiology. 1988; 71(4):289–295. [PubMed: 2454794]
31. Aoyagi M, et al. Effects of aging on amplitude-modulation following response. Acta oto-laryngologica. Supplementum. 1994; 511:15–22.
32. Rojas DC, et al. Development of the 40Hz steady state auditory evoked magnetic field from ages 5 to 52. Clinical neurophysiology : official journal of the International Federation of Clinical Neurophysiology. 2006; 117(1):110–117. [PubMed: 16316780]
33. Cho RY, et al. Development of sensory gamma oscillations and cross-frequency coupling from childhood to early adulthood. Cerebral cortex. 2015; 25(6):1509–1518. [PubMed: 24334917]
34. Poulsen C, Picton TW, Paus T. Age-related changes in transient and oscillatory brain responses to auditory stimulation during early adolescence. Developmental science. 2009; 12(2):220–235. [PubMed: 19143796]
35. Herdman AT, et al. Determination of activation areas in the human auditory cortex by means of synthetic aperture magnetometry. NeuroImage. 2003; 20(2):995–1005. [PubMed: 14568469]
36. Ross B, Herdman AT, Pantev C. Right hemispheric laterality of human 40 Hz auditory steady-state responses. Cerebral cortex. 2005; 15(12):2029–2039. [PubMed: 15772375]
37. Ross B, Picton TW, Pantev C. Temporal integration in the human auditory cortex as represented by the development of the steady-state magnetic field. Hearing research. 2002; 165(1-2):68–84. [PubMed: 12031517]
38. Lord C, et al. The autism diagnostic observation schedule-generic: a standard measure of social and communication deficits associated with the spectrum of autism. Journal of autism and developmental disorders. 2000; 30(3):205–223. [PubMed: 11055457]
39. Lord C, Rutter M, Le Couteur A. Autism Diagnostic Interview-Revised: a revised version of a diagnostic interview for caregivers of individuals with possible pervasive developmental disorders. Journal of autism and developmental disorders. 1994; 24(5):659–685. [PubMed: 7814313]
40. Taulu S, Simola J. Spatiotemporal signal space separation method for rejecting nearby interference in MEG measurements. Physics in medicine and biology. 2006; 51(7):1759–1768. [PubMed: 16552102]
41. Roberts TP, et al. MEG detection of delayed auditory evoked responses in autism spectrum disorders: towards an imaging biomarker for autism. Autism research : official journal of the International Society for Autism Research. 2010; 3(1):8–18. [PubMed: 20063319]
42. Jacobson GP, Fitzgerald MB. Auditory evoked gamma band potential in normal subjects. Journal of the American Academy of Audiology. 1997; 8(1):44–52. [PubMed: 9046068]

43. Pantev C. Evoked and induced gamma-band activity of the human cortex. Brain topography. 1995; 7(4):321–330. [PubMed: 7577330]
44. Scherg M, Von Cramon D. Two bilateral sources of the late AEP as identified by a spatio-temporal dipole model. Electroencephalography and clinical neurophysiology. 1985; 62(1):32–44. [PubMed: 2578376]
45. Ponton C, Eggermont JJ, Khosla D, Kwong B, Don M. Maturation of human central auditory system activity: separating auditory evoked potentials by dipole source modeling. Clinical neurophysiology : official journal of the International Federation of Clinical Neurophysiology. 2002; 113(3):407–420. [PubMed: 11897541]
46. Hoechstetter K, et al. BESA source coherence: a new method to study cortical oscillatory coupling. Brain topography. 2004; 16(4):233–238. [PubMed: 15379219]
47. Berg P, Scherg M. A multiple source approach to the correction of eye artifacts. Electroencephalography and clinical neurophysiology. 1994; 90(3):229–241. [PubMed: 7511504]
48. Lins OG, Picton TW, Berg P, Scherg M. Ocular artifacts in recording EEGs and event-related potentials. II: Source dipoles and source components. Brain topography. 1993; 6(1):65–78. [PubMed: 8260328]
49. Scherg M, Ebersole JS. Models of brain sources. Brain topography. 1993; 5(4):419–423. [PubMed: 8357717]
50. Scherg M, Ille N, Bornfleth H, Berg P. Advanced tools for digital EEG review: virtual source montages, whole-head mapping, correlation, and phase analysis. Journal of clinical neurophysiology : official publication of the American Electroencephalographic Society. 2002; 19(2):91–112. [PubMed: 11997721]
51. Papp N, Ktonas P. Critical evaluation of complex demodulation techniques for the quantification of bioelectrical activity. Biomedical sciences instrumentation. 1977; 13:135–145. [PubMed: 871500]
52. Edgar JC, et al. Neuromagnetic Oscillations Predict Evoked-Response Latency Delays and Core Language Deficits in Autism Spectrum Disorders. Journal of autism and developmental disorders. 2013
53. Edgar JC, et al. Superior temporal gyrus spectral abnormalities in schizophrenia. Psychophysiology. 2008; 45(5):812–824. [PubMed: 18665866]
54. Fischl B, Dale AM. Measuring the thickness of the human cerebral cortex from magnetic resonance images. Proceedings of the National Academy of Sciences of the United States of America. 2000; 97(20):11050–11055. [PubMed: 10984517]
55. Edgar JC, et al. Temporal and frontal cortical thickness associations with M100 auditory activity and attention in healthy controls and individuals with schizophrenia. Schizophrenia research. 2012; 140(1-3):250–257. [PubMed: 22766129]
56. Constantino JN, et al. Validation of a brief quantitative measure of autistic traits: comparison of the social responsiveness scale with the autism diagnostic interview-revised. Journal of autism and developmental disorders. 2003; 33(4):427–433. [PubMed: 12959421]
57. Shahin AJ, Roberts LE, Miller LM, McDonald KL, Alain C. Sensitivity of EEG and MEG to the N1 and P2 auditory evoked responses modulated by spectral complexity of sounds. Brain topography. 2007; 20(2):55–61. [PubMed: 17899352]
58. Bohorquez J, Ozdamar O. Generation of the 40-Hz auditory steady-state response (ASSR) explained using convolution. Clinical neurophysiology : official journal of the International Federation of Clinical Neurophysiology. 2008; 119(11):2598–2607. [PubMed: 18818122]
59. Yvert B, Crouzeix A, Bertrand O, Seither-Preisler A, Pantev C. Multiple supratemporal sources of magnetic and electric auditory evoked middle latency components in humans. Cerebral cortex. 2001; 11(5):411–423. [PubMed: 11313293]
60. Pantev C, et al. Relationship of transient and steady-state auditory evoked fields. Electroencephalography and clinical neurophysiology. 1993; 88(5):389–396. [PubMed: 7691563]
61. Ponton CW, Moore JK, Eggermont JJ. Prolonged deafness limits auditory system developmental plasticity: evidence from an evoked potentials study in children with cochlear implants. Scandinavian audiology. Supplementum. 1999; 51:13–22. [PubMed: 10803910]

62. Moore JK, Guan YL. Cytoarchitectural and axonal maturation in human auditory cortex. Journal of the Association for Research in Otolaryngology : JARO. 2001; 2(4):297–311. [PubMed: 11833605]

63. Moore JK, Linthicum FH Jr. The human auditory system: a timeline of development. International journal of audiology. 2007; 46(9):460–478. [PubMed: 17828663]

64. Gaetz W, Macdonald M, Cheyne D, Snead OC. Neuromagnetic imaging of movement-related cortical oscillations in children and adults: age predicts post-movement beta rebound. NeuroImage. 2010; 51(2):792–807. [PubMed: 20116434]

65. Berchicci M, et al. Development of mu rhythm in infants and preschool children. Developmental neuroscience. 2011; 33(2):130–143. [PubMed: 21778699]

66. Klimesch W. EEG alpha and theta oscillations reflect cognitive and memory performance: a review and analysis. Brain research. Brain research reviews. 1999; 29(2-3):169–195. [PubMed: 10209231]

67. Edgar JC, et al. Resting-State Alpha in Autism Spectrum Disorder and Alpha Associations with Thalamic Volume. Journal of autism and developmental disorders. 2014

68. Ehlers CL, Wills DN, Desikan A, Phillips E, Havstad J. Decreases in energy and increases in phase locking of event-related oscillations to auditory stimuli occur during adolescence in human and rodent brain. Developmental neuroscience. 2014; 36(3-4):175–195. [PubMed: 24819672]

69. Huttenlocher PR, Dabholkar AS. Regional differences in synaptogenesis in human cerebral cortex. The Journal of comparative neurology. 1997; 387(2):167–178. [PubMed: 9336221]

70. Gao WJ, Newman DE, Wormington AB, Pallas SL. Development of inhibitory circuitry in visual and auditory cortex of postnatal ferrets: immunocytochemical localization of GABAergic neurons. The Journal of comparative neurology. 1999; 409(2):261–273. [PubMed: 10379919]

71. Gogtay N, et al. Dynamic mapping of human cortical development during childhood through early adulthood. Proceedings of the National Academy of Sciences of the United States of America. 2004; 101(21):8174–8179. [PubMed: 15148381]

72. Port RG, Ku M, Murray R, Blaskey L, Roberts TPL. Confirmation of M100 latency and gamma-band response maturation in healthy children and children with ASD using longitudinal study design. International Society for Autism Research. 2015

73. Gross J, et al. Good practice for conducting and reporting MEG research. NeuroImage. 2013; 65:349–363. [PubMed: 23046981]

74. Ross B, Borgmann C, Draganova R, Roberts LE, Pantev C. A high-precision magnetoencephalographic study of human auditory steady-state responses to amplitude-modulated tones. The Journal of the Acoustical Society of America. 2000; 108(2):679–691. [PubMed: 10955634]

75. Hipp JF, Siegel M. Dissociating neuronal gamma-band activity from cranial and ocular muscle activity in EEG. Frontiers in human neuroscience. 2013; 7:338. [PubMed: 23847508]

76. Lazzouni L, Ross B, Voss P, Lepore F. Neuromagnetic auditory steady-state responses to amplitude modulated sounds following dichotic or monaural presentation. Clinical neurophysiology : official journal of the International Federation of Clinical Neurophysiology. 2010; 121(2):200–207. [PubMed: 20005163]

77. Ross B, Picton TW, Herdman AT, Pantev C. The effect of attention on the auditory steady-state response. Neurology & clinical neurophysiology : NCN. 2004; 2004:22. [PubMed: 16012602]

78. Tiitinen H, et al. Selective attention enhances the auditory 40-Hz transient response in humans. Nature. 1993; 364(6432):59–60. [PubMed: 8316297]

79. Herdman AT. Neuroimaging evidence for top-down maturation of selective auditory attention. Brain topography. 2011; 24(3-4):271–278. [PubMed: 21499933]

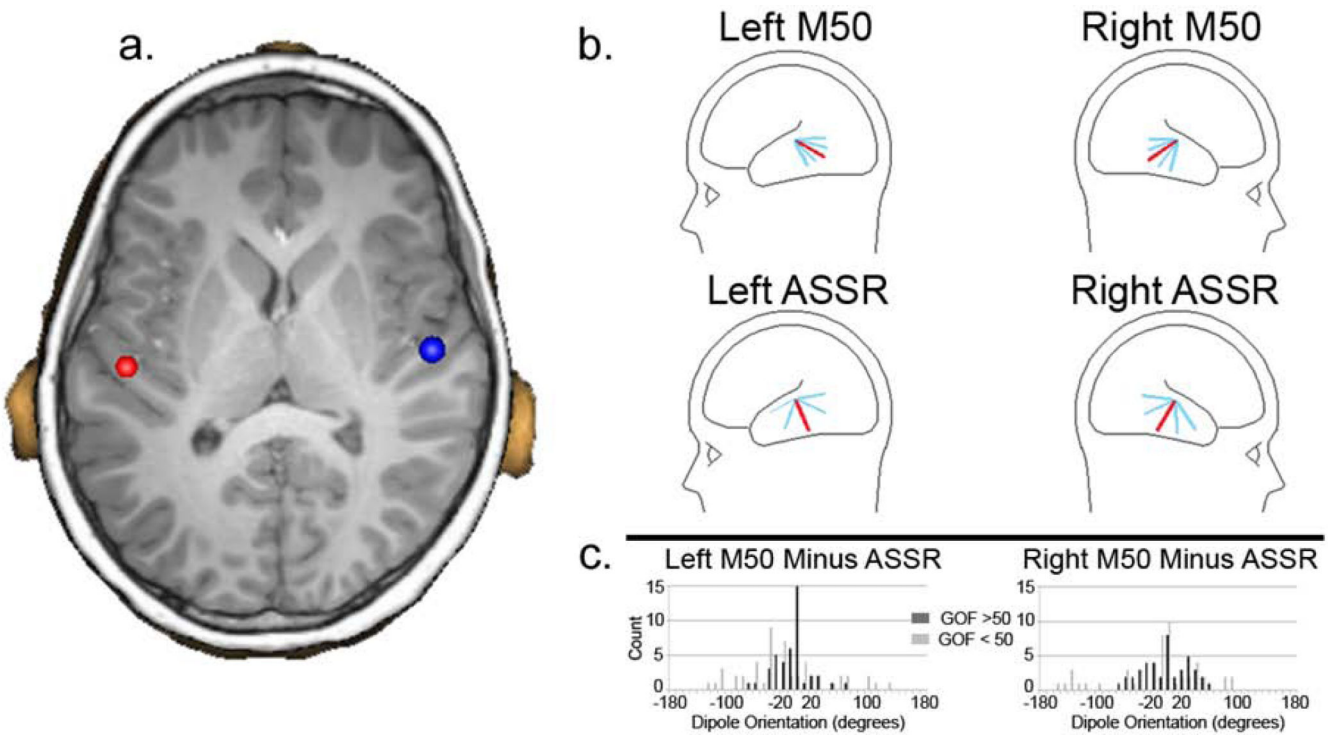

1.

1a) Coronal slice showing placement of dipole sources in left and right Heschl's Gyrus. As detailed in the 'Results', a main effect of Hemisphere showed more posterior dipole placements on the left than right (4.09 mm y-axis difference). 1b) Top row: M50 dipole orientation for the left and right hemisphere (total sample) with the average M50 dipole orientation in red and with 1 and 2 standard deviation bars in blue. Bottom row: 40 Hz ASSR dipole. For both the M50 and 40 Hz ASSR, the sagittal dipole angle was examined as this best captures the variability in the tangentially oriented STG M50 and 40 Hz ASSR dipole orientations. 1c) For each participant the difference in the M50 and 40 Hz ASSR dipole orientation was computed for the left and right hemisphere. The histogram shows orientation difference values for participants with better GOF (> 60%; dark gray) and worse GOF (<50%; light gray), and indicates greater similarly (tighter clustering) in individuals with better GOF values, with no participant with a better GOF exceeding a 80 degree (left) or 50 degree (right) difference.

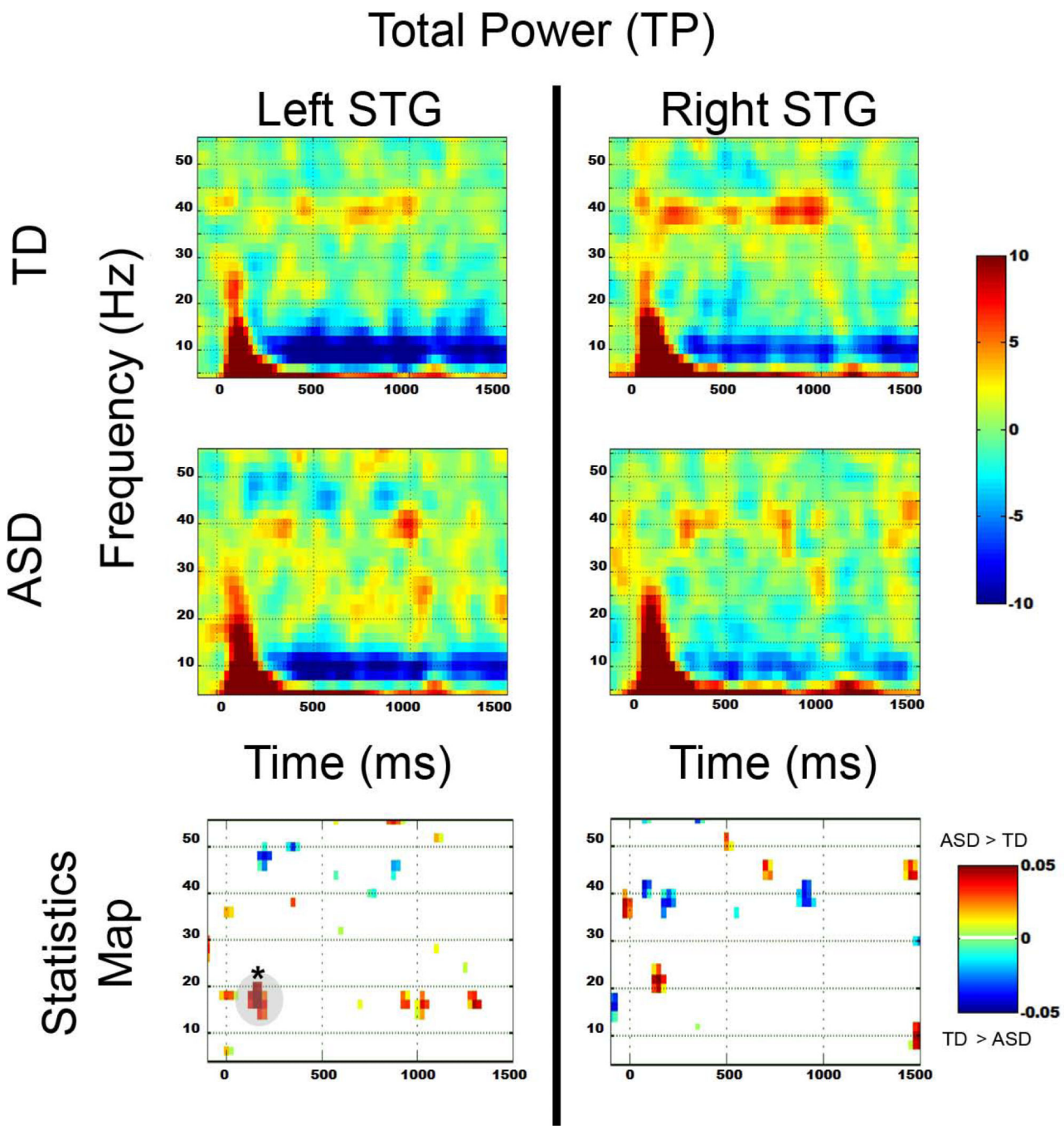

2.

Total power TD (top row) and ASD (middle row) and uncorrected p-value plots (bottom row) comparing TD and ASD for each frequency. In the statistics map, time-frequency voxels significant at $p < 0.05$ are shown, with regions surviving familywise correction highlighted in gray and with a '*'.

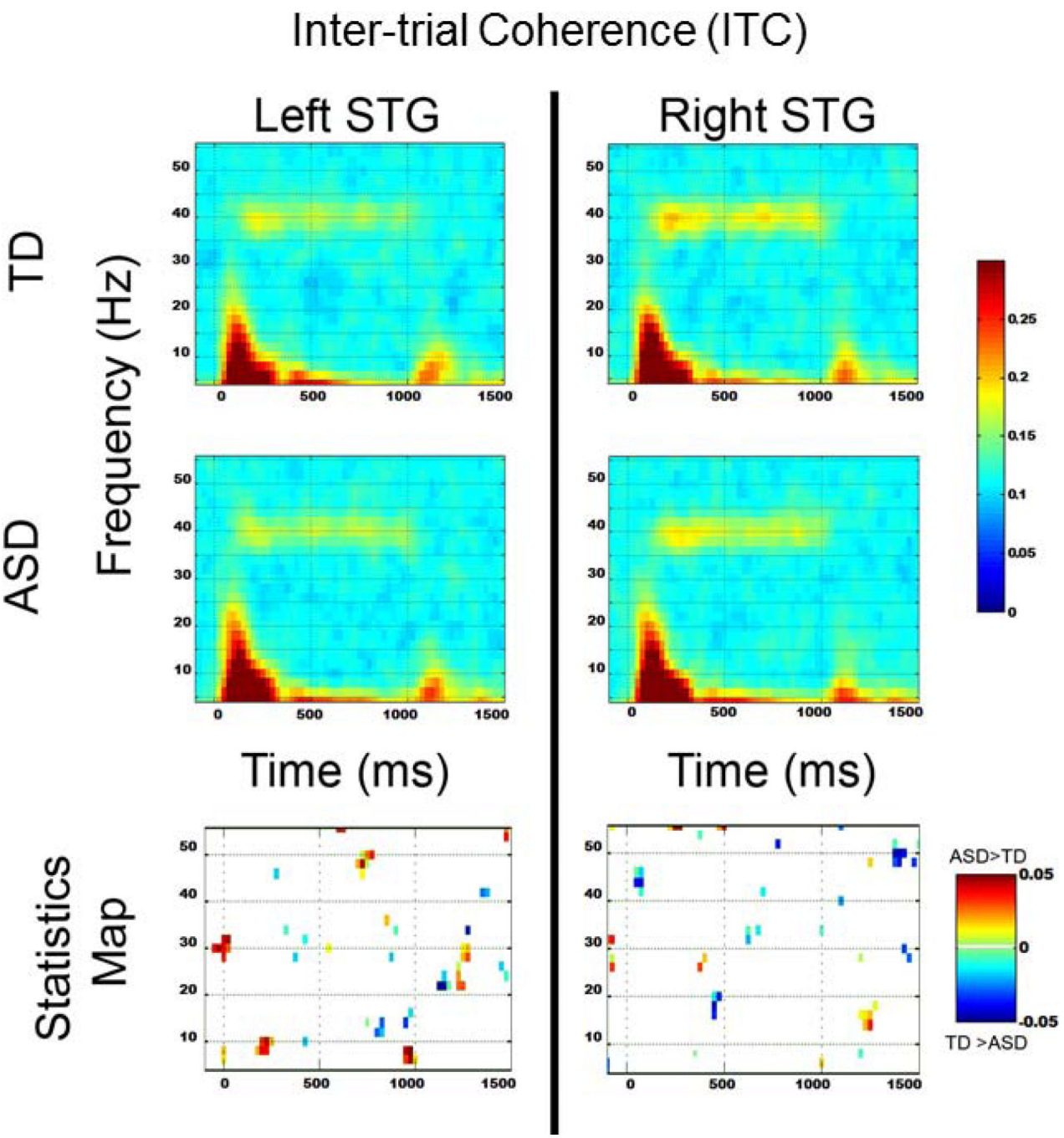

3.

Inter-trial coherence TD (top row) and ASD (middle row) and uncorrected p-value plots (bottom row) comparing TD and ASD for each frequency. In the statistics map, time-frequency voxels significant at $p < 0.05$ are shown.

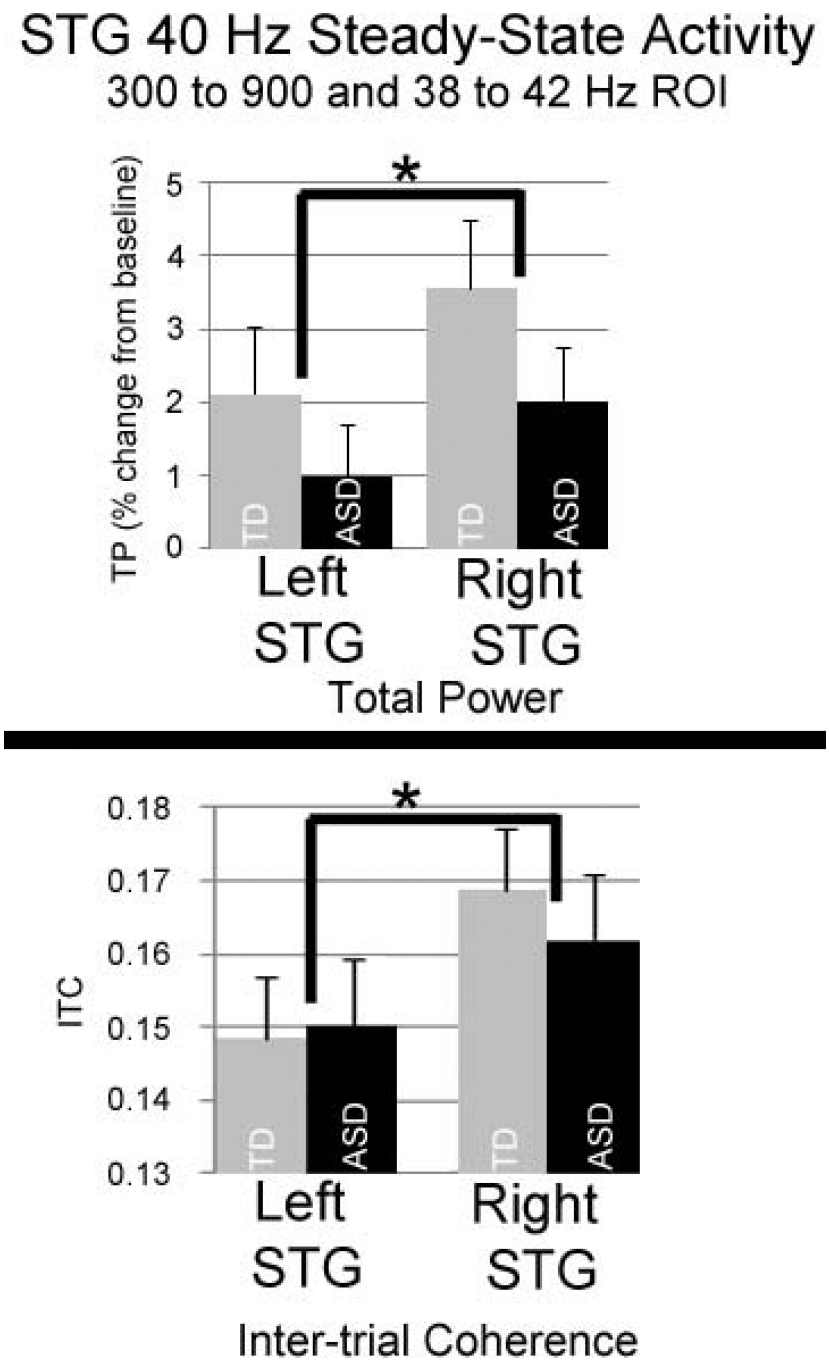

4.

Bar graphs show mean and standard error 40 Hz ASSR TP (top) and ITC (bottom) values (TP and ITC averaged across a 300 to 900 ms and 38 to 42 Hz region of interest) for each group and each hemisphere. For TP and ITC, there was only a significant main effect of Hemisphere (right > left).

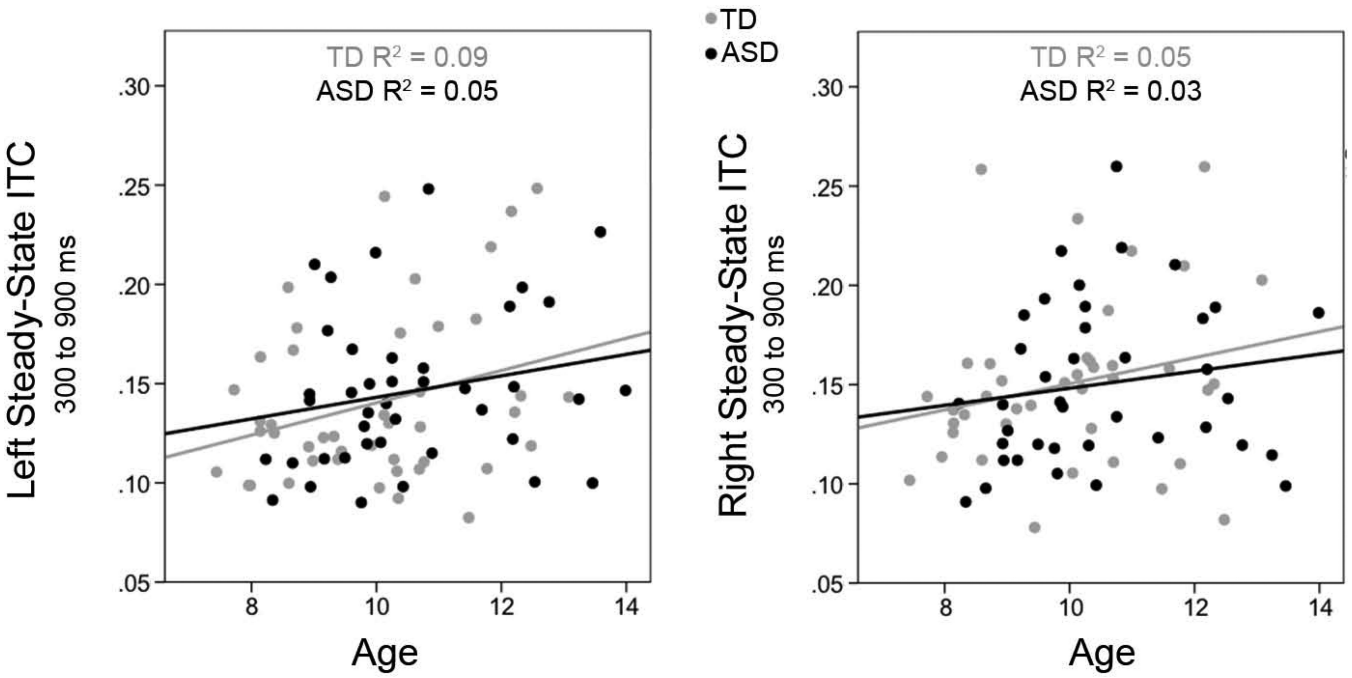

5.

5a) Scatterplots show associations between age and ITC for TD (light grey) and ASD (black) for each hemisphere. In both hemispheres a main effect of Age indicated a ~0.01/ year increase in ITC.

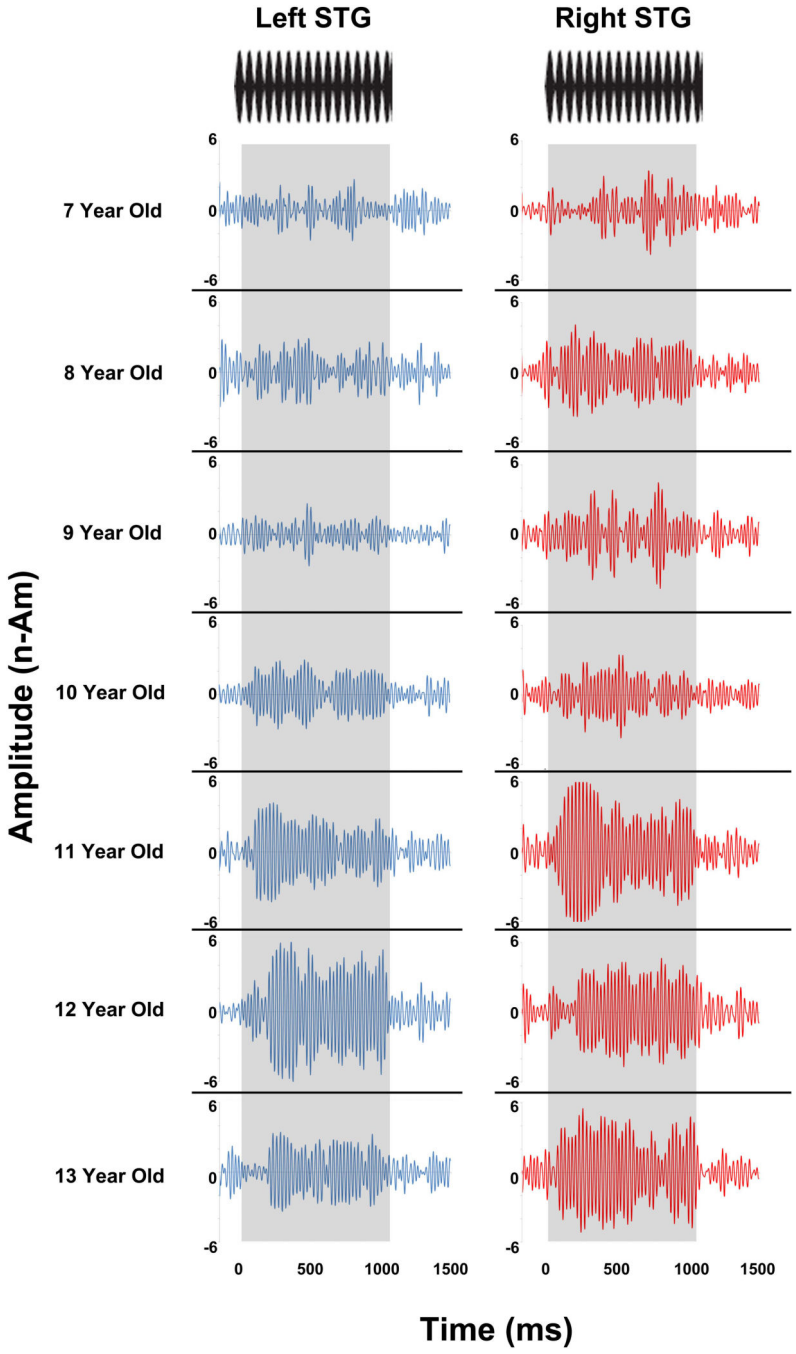

6.

Left and right 40 Hz ASSR STG evoked timecourses shown for a representative child from ages 7 to 13 years (dipoles anatomically constrained to left and right Heschl's Gyrus). Time is shown on the x axis and source strength on the y axis. Steady-state stimuli are shown at the top, with the duration of the steady-state tone highlighted in gray. Whereas older children (11- to 13-years-old) showed a left and right STG 40 Hz ASSR (e.g., very clear

offset response), STG 40 Hz auditory steady-state activity was much less evident in the younger children (7- to 10-years-old).

1

Demographic information

	TD (N = 48)		ASD (N = 42)			
	mean	**SD**	**mean**	**SD**	**t-value**	**p-value**
Age	10.1	1.5	10.6	1.5	1.74	> 0.05
SRS	40.8	6.3	75.3	11.6	17.81	< 0.01
DASII GCA	112.0	12.45	106.6	22.67	1.43	> 0.05